Three-Dimensional Echocardiography based Evaluation of Right Ventricular Remodeling in Patients with Pressure Overload

Francesco Maffessanti[1,2], Karima Addetia[1], Megan Yamat[1], Lynn Weinert[1], Roberto M Lang[1], Victor Mor-Avi[1]

[1] Section of Cardiology, Department of Medicine, University of Chicago, Chicago, IL, USA
[2] Center for Computational Medicine in Cardiology (CCMC), Institute of Computational Science, Università della Svizzera italiana, Lugano, Switzerland

Abstract

Although 3D echocardiography (3DE) allows imaging of right ventricular (RV) morphology, regional RV remodeling has not been evaluated using 3DE. We developed a technique to quantify regional RV shape and tested its ability to characterize RV shape in normal subjects and in patients with RV pressure overload.

Transthoracic 3DE images were acquired in 54 subjects (39 patients with pulmonary artery hypertension, PAH, and 15 normal controls, NL). 3D RV surfaces were reconstructed at end-diastole and end-systole (ED, ES) and analyzed using custom software to calculate 3D mean curvature of the inflow and outflow tracts, apex and body (both divided into free-wall and septum).

Septal segments in NLs were characterized by concavity (curvature<0) in ED and slight convexity (curvature>0) in ES. Conversely, the septum remained convex throughout the cardiac cycle in PAH. In the NL group, the body free-wall transitioned from a convex surface to a more flattened surface during contraction, while the convexity of the apex free-wall increased. In contrast, in PAH, both RV free-wall segments remained equally convex throughout the cardiac cycle.

Curvature analysis using 3DE allows quantitative evaluation of RV remodeling, which could be used to track differential changes in regional RV shape, as a way to assess disease progression or regression.

1. Introduction

Alterations in cardiac chambers' shape occur as part of the remodeling process that follows altered hemodynamic loading conditions and subsequent myocyte injury. While left ventricular (LV) morphology has been extensively studied and it is now accepted that LV shape conveys valuable physiologic information that is independent of size and function, little is known about right ventricular (RV) remodeling. This is mainly due to the complex RV shape that cannot be described using 2D images, unless introducing geometrical assumptions and using approximation. The availability of 3D transthoracic echocardiography (TTE) may overcome this limitation, as it allows acquisition of truly 3D dynamic datasets of the RV cavity throughout the cardiac cycle.

Accordingly, we hypothesized that RV pathology would affect RV shape, and analysis of 3D TTE images would allow us to quantitatively detect the changes occurring with the remodeling process. To test this hypothesis, we developed a technique for quantitative analysis of RV regional curvature from 3D TTE-derived dynamic endocardial surfaces and tested it in patients with RV pressure overload due to pulmonary artery hypertension (PAH) and in normal (NL) subjects.

2. Methods

2.1. Patient population

We enrolled 39 consecutive patients with severe PAH (5 men; 33 women; age 50±15 years) and 15 normal subjects (6 men; 9 women; age 50±17 years). All study subjects underwent a complete 2D and 3D TTE examination. Severe PAH was defined by systolic pulmonary arterial pressures >50 mmHg (measured by Doppler echocardiography), associated with systolic and diastolic septal flattening. NL group included subjects with no coronary artery disease and on no medications, with a normal 2D TTE study. The Institutional Review Board approved the study.

2.2. Echocardiographic imaging

Comprehensive 2D and color Doppler evaluation was performed using an iE33 imaging system with an S5 transducer (Philips Healthcare, Andover, MA). Based on the current recommendations [1,2], the following measurements were taken: 1) LV ejection fraction; 2)

maximal RV tricuspid annular plane systolic excursion (TAPSE, in mm); 3) maximal RV systolic excursion velocity (S', in cm/s); 4) right atrial (RA) area (cm^2); 5) peak TR gradient (mmHg). Finally, systolic pulmonary arterial pressure (mmHg) was estimated using the tricuspid regurgitation (TR) gradient and adding an approximation of RA pressure based on inferior vena cava size and collapsibility [1].

3D TTE images of the RV were acquired from a modified apical 4-chamber, using the same imaging system equipped with a matrix array transducer (X5-1), in the full-volume mode, using ECG gating over 4 consecutive cardiac cycles during a single breath-hold. Digital 3D TTE datasets were analyzed using commercial software (4D RV-Function 1.1, TomTec Imaging Systems, Unterschleissheim, Germany) to quantify RV end-diastolic and end-systolic (ED, ES) volumes and ejection fraction. ED and ES frames were identified as the frames depicting the largest and the smallest RV cavity, respectively. Analysis required manual initialization of the contours in both ED and ES frames in the apical 4-chamber, coronal, and sagittal views. 3D renderings of the RV endocardial surface were then automatically generated and exported as triangular meshes (Figure 1, left).

2.3. 3D curvature analysis

Custom software was used for the analysis of regional RV endocardial curvature. For each node of the mesh, a quadratic polynomial function was locally fitted to approximate the 2nd order neighborhood of the node with a smooth surface [3] and obtain a mathematical representation of the local surface (Figure 1).

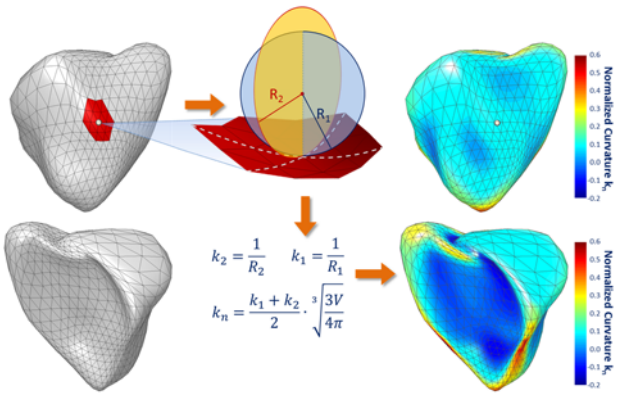

Figure 1. Schematic of the calculation of 3D curvature. See text for details.

Then, two values were analytically derived for each node: the maximum curvature k_1, equivalent to the inverse of the radius R1 of the smallest circle fitting the surface at that particular node (Figure 1, light blue circle), and the curvature k_2 as the inverse radius of the fitting circle (Figure 1, orange circle) in the perpendicular direction. Then, the mean 3D curvature k was obtained by averaging, for each node, the two values k_1 and k_2.

In order to compensate for changes in RV curvature secondary to changes in RV volume (i.e. for a pure scaling transformation that does not affect the local RV shape), the value of 3D curvature k for each node was normalized by mean regional RV curvature, defined as the $(\text{mean radius})^{-1}$. Then, the mean radius was obtained from the regional RV volume assuming the region being spherical.

Of note, zero curvature defines a flat surface, whereas a positive or negative curvature depicts convexity or concavity, respectively. The more positive/negative the curvature, the more convex/concave the surface.

The RV surface was divided into six regions (Figure 2): 1) inflow tract (RVIT); 2) outflow tract (RVOT); 3) and 4) septal and free-wall body; 5) and 6) septal and free-wall apex. The regional 3D curvature k_n was obtained by averaging the values of all points within the region.

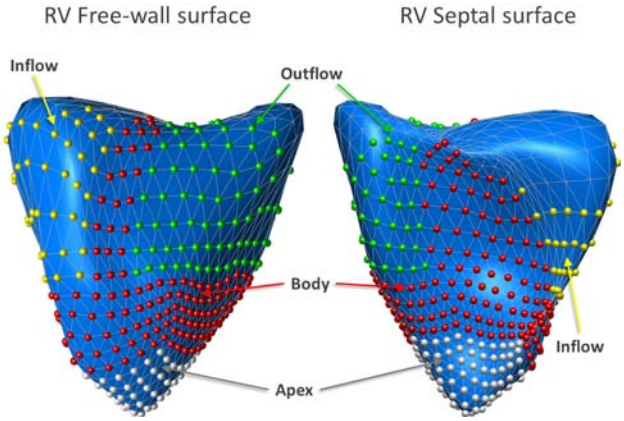

Figure 2. Subdivision of the RV surface into regions. See text for details.

To test the performance of the algorithm for 3D curvature computation, a series of computer-simulated ellipsoids were generated (Figure 3). We considered: A) three spheres, S1 to S3, with different radii; B) three ellipsoids: S4 and S5 with transverse and longitudinal circular cross-sections, respectively, and S6 with three different radii. All the test ellipsoids had the same number of vertices (961) and faces (1740). 3D absolute curvature was computed for each node.

2.4. Statistical analysis

Continuous variables were summarized as mean ± SD, while categorical variables were presented as absolute numbers and percentages, unless otherwise stated. Measurements for PAH and NL were compared using unpaired t-tests, while end-diastolic and end-systolic

values were compared using paired t-tests. Statistical significance was defined as $p \leq 0.05$.

3. Results

Table 1 shows the echocardiographic characteristics for the NL and PAH groups. On average, the RV ejection fraction was moderately-to-severely reduced in PAH patients, while RV volumes were significantly larger.

Table 1. RV echocardiographic characteristics of the study groups.

Text	NL	PAH	p-val
EF (%)	54±4	25±9	<0.01
EDV (mL)	104±31	259±116	<0.01
ESV (mL)	48±16	198±100	<0.01

3.1. Algorithm validation

As shown in Figure 3, the curvature pattern in the 3 perfect spheres S1, S2 and S3 was uniform and equal to the inverse of the radius (k=1/1=1 for S1, k=1/1.5=0.67 for S2 and k=1/2=0.5 for S3).

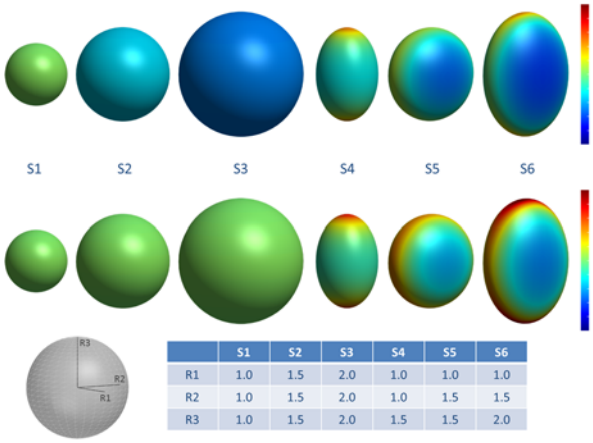

	S1	S2	S3	S4	S5	S6
R1	1.0	1.5	2.0	1.0	1.0	1.0
R2	1.0	1.5	2.0	1.0	1.5	1.5
R3	1.0	1.5	2.0	1.5	1.5	2.0

Figure 3. Simulated ellipsoids (S1 to S6, left to right) used for validating the 3D curvature algorithm are color-coded based on local absolute (top) and indexed (mid) 3D curvature values. The corresponding three main radii, are shown in the table below. See text for details.

After normalization, k_n values for the spheres S1 to S3 became equal to 1, in keeping with the fact that indexed curvature describes the local similarity of a surface to a sphere having the same volume. S4 showed increasing values of curvature along the longitudinal direction, while the value (coded in color) in the transverse plane was uniform, in accordance with the fact that the cross-section was circular. Similar observations can be made for S5, but in the transverse rather than in the longitudinal direction. In the case of S6, no symmetry in curvature distribution was found, as the 3 radii were different, and the color-coded "pebble-shaped" surface clearly showed a flatter region (blue), with more intense (curved region) longitudinally, as expected. After normalization, k_n was able to clearly differentiate the local shape of the ellipsoids S4-S6 from the spheres S1-S3.

3.2. RV morphology in controls

Mean regional curvature values for the normal right ventricle are shown in Table 2. Septal segments (both apical and body) were characterized by concavity (negative values) at end-diastole and slight convexity (positive values) at end-systole. In keeping with the bellows-like action of normal RV contraction, the free-wall body segment becomes less convex when transitioning from end-diastole to end-systole, while the apical free-wall progresses from a less convex surface at end-diastole to a more convex one at end-systole.

3.2. RV remodeling in PAH

With respect to regional curvature indices, the RVOT was more convex (rounded) in PAH compared to normal (Table 2 and Figure 4). The septum was more convex, (i.e. bulging into the left ventricle) in PAH, compared to controls (Table 2). No patient in the PAH group had septal concavity at any time throughout the cardiac cycle. Of note, the PAH group demonstrated loss of the bellows-like action seen in the control group with the free-wall segments (apical and body), remaining equally convex throughout at ED and ES.

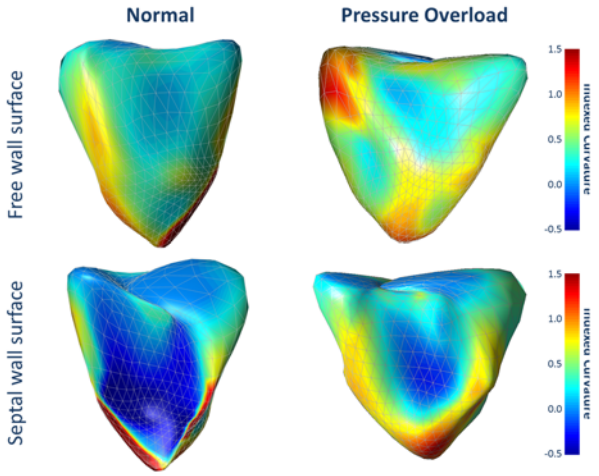

Figure 4. Color-coded map of 3D curvature values in a normal (left) and in a PAH right ventricle (right) at end-diastole.

Table 2. RV echocardiographic characteristics of the study groups. *: p<0.05 NL vs PAH, unpaired t-test.

	End-Diastole		End-Systole	
	NL	PAH	NL	PAH
Volume (ml)				
Global	103±31	258±116*	48 ±15	203±102*
Apex	5±2	32±18*	5±1	30±16*
Body	22±8	68±39*	11±4	58±34*
RVIT	49±16	102±34*	20±7	70±30*
RVOT	26±10	57±30*	12±4	44±24*
Curvature				
Apex	0.51±0.16	0.73±0.08*	0.68±0.08	0.73±0.07*
Body	0.42±0.08	0.53±0.05*	0.40±0.06	0.54±0.04*
RVIT	0.79±0.07	0.81±0.07	0.71±0.06	0.77±0.06*
RVOT	0.47±0.11	0.57±0.10*	0.45±0.09	0.56±0.09*
Free wall body	0.69±0.09	0.56±0.06*	0.56±0.06	0.56±0.05
Free wall apex	0.71±0.19	0.71±0.08	0.87±0.11	0.70±0.08*
Septal body	-0.09±0.13	0.49±0.18*	0.07±0.10	0.50±0.13*
Septal apex	-0.08±0.10	0.82±0.29*	0.10±0.15	0.87±0.24*

4. Discussions and conclusions

To date, no method exists to evaluate changes in RV shape, although different methods are used to assess RV size and function. This is the first study to assess 3D echocardiography derived global and regional RV shape indices in normal subjects and in patients with pressure overload due to PAH. We demonstrated that in PAH, right ventricles exhibit differences in regional curvature evident in the outflow tract, septal and apical free-wall regions, when compared with normal right ventricles. In PAH, the outflow tract was more round, and, in the septum, both body and apical portions were more convex, i.e. bulging into the left ventricle at both end-diastole and end-systole, with a more flattened apical free wall. Additionally, in PAH, the right ventricle lost the dynamic behavior of the free wall that was seen in the normal ventricles. In normal controls, the free-wall body segment became less convex, while the free-wall apex changed to a more convex surface from end-diastole to end-systole. In contrast, in PAH, both RV free-wall segments (apical and body) remained equally convex throughout the cardiac cycle.

This analysis provided new insight into normal RV contraction by quantifying differences between pressure-overloaded versus normal right ventricles. This methodology could potentially be used to better understand RV physiology and remodeling in a variety of disease states, and might be useful in the follow-up of RV response to therapy. Future studies are warranted to determine the relationship between RV shape and

References

[1] Rudski LG, Lai WW, Afilalo J, et al. Guidelines for the echocardiographic assessment of the right heart in adults: a report from the American Society of Echocardiography endorsed by the European Association of Echocardiography, a registered branch of the European Society of Cardiology, and the Canadian Society of Echocardiography. J Am Soc Echocardiogr 2010; 23:685-713.

[2] Lang RM, Badano LP, Mor-Avi V, et al. Recommendations for Cardiac Chamber Quantification by Echocardiography in Adults: An Update from the American Society of Echocardiography and the European Association of Cardiovascular Imaging. J Am Soc Echocardiogr 2014; 28:1-39 .

[3] Garimella RV, Swartz BK: Curvature Estimation for Unstructured Triangulations of Surfaces. Los Alamos, New Mexico, Los Alamos National Library, 2003.

Address for correspondence:

Francesco Maffessanti, PhD
University of Chicago Medical Center, M.C. 5084
5841 S Maryland Ave., 60637 Chicago, IL, USA
fmaffe@gmail.com